Chapter – 3

Synthesis, Characterization and catalytic applications of chitosan-ironoxide nanocomposite for degradation of Individual dyes and binary mixture of dyes

3.1 Introduction

Nano sized magnetic particles are important materials not only in the field of magnetic recording but also in the areas of biological and medical applications such as drug carrier [1, 2], drug release [3], cancer therapy [4], hyperthermia, magnetic separation and magnetic resonance imaging (MRI). The most important is its non-toxicity and high biocompatibility which make these magnetic materials also amenable for various applications in environmental treatment methods.

Fenton's process of oxidation for treatment of waste water pollutants is considered as one of the most effective AOP due to the high oxidation potential of the hydroxyl radical produced. However, this fenton's process produces a large amount of sludge and so alternatively various catalysts are produced by immobilizing the iron oxide materials onto a solid support [5-10]. Combination of nanomagnetic and porous materials couldalso further improve the degradation process due to its high surface area and high separation efficiency (11-16)

Many methods for the synthesis of nanoparticles have been developed like sol–gel process, microemulsion, sputtering, thermal decomposition [17–20], etc. However, the coprecipitation method is still the most popularly adopted method due to its simplicity.

Iron oxides (either Fe_3O_4 or γ-Fe_2O_3) are usually prepared using a stoichiometric mixture of ferrous and ferric salts in aqueous medium. The chemical reaction of Fe_3O_4 formation may be written as.

$$\mathbf{Fe^{2+}+2Fe^{3+}+8OH^{-}\rightarrow Fe_3O_4+4H_2O} \qquad \text{.....eq. (1)}$$

According to the thermodynamics of this reaction, complete precipitation of Fe_3O_4 should be expected at a pH between 8 and 14, with a stoichiometric ratio of 2:1 (Fe^{3+}/Fe^{2+}) in a non-oxidizing oxygen environment [21]. However, magnetite (Fe_3O_4) is not very stable and is sensitive to oxidation. Magnetite is transformed into maghemite (γFe_2O_3) in the presence of oxygen.

$$Fe_3O_4+2H^+ \rightarrow \gamma\text{-}Fe_2O_3+Fe^{2+}+H_2O \quad \text{.....eq. (2)}$$

Oxidation in air is not the only way to transform magnetite (Fe_3O_4) into maghemite (γ-Fe_2O_3). Various electron or ion transfers depending upon the pH of the suspension are involved, according to eq 2. Under acidic and anaerobic conditions, surface Fe^{2+}ions are desorbed as hexa-aqua complexes in solution, whereas, under basic conditions, the oxidation of magnetite involves the oxidation-reduction of the surface of magnetite. The main advantage of the coprecipitation process is that a large amount of nanoparticles can be synthesized. However, the control of particle size distribution is limited [22-27]. A wide variety of factors can be adjusted in the synthesis of iron oxide nanoparticles to control size, magnetic characteristics, or surface properties [28, 29]. The size and shape of the nanoparticles can be customized by adjusting pH, ionic strength, temperature, nature of the salts (perchlorates, chlorides, sulfates, and nitrates), or the Fe^{2+}/Fe^{3+}concentration ratio. [30]. The addition of chelating organic anions (carboxylate orhydroxy carboxylate ions, such as citric, gluconic or oleic acid) or polymer surface complexing agents (dextran, carboxy dextran, starch or polyvinyl alcohol) during the formation of magnetite can help to control the size of the nanoparticles. The first controlled preparation of super-paramagnetic iron oxide particles using alkaline precipitation of $FeCl_3$ and $FeCl_2$was performed by Massart [31]. However with modulation of different parameters like pH, base other cations and Fe^{2+}/Fe^{3+}ratio it was possible to obtain particles with a size ranging from 16.6 to 4.2 nm [32]. The particles can be dispersed in either aqueous media or nonpolar liquids, such as oil or organic solvents, allowing for the preparation of magnetic emulsion, capsules, and vesicles [33-35]. Coating by a wide range of monomeric species, such as aminoacids, hydroxyacids (citric, tartaric, and gluconic acids) [36], hydroxamate (arginine hydroxamate) [37], Dimercapto succinic acid (DMSA) [38, 39], or phosphoryl choline [40] have also been reported. Several researchers have studied the possibility of using alkane sulphonic and alkane phosphonic acid surfactants as efficient binding ligands on the surface of Fe_2O_3 nanoparticles andasstabilizers for particledispersioninorganic solvents [41-44].

The Fe^{2+}/Fe^{3+} ratio and concentration played a important role on the composition, size, morphology and magnetic properties of co-precipitated nanoscale particles and also could lead to different forms of iron oxide [45, 46].

The size and morphologyof the particles during the co-precipitation process are manipulated by the use of templates. For instance, uniformly sized magnetite nanoparticles were synthesized by the high-temperature reaction of $Fe(acac)_3$ in octyl ether and oleic acid or lauric acid or a mixture of four solvents and ligands, namely, phenyl ether, 1, 2hexadecanediol, oleic acid, and oleylamine. Even thoughhighly crystalline and uniformly sized magnetic nanoparticles are reported to be produced by these methods they have various drawbacks, as they involve the use of expensive and toxic reagents, complicated synthetic steps, and high reaction temperatures [47]. Functional groups, including carboxylates, phosphates, and sulfates, are known to bind to the surface of magnetites [48-49].

Synthetic control of morphology and composition of the nanoparticles has been achieved using a variety of wet chemical methods [50, 51]. Polymers as stabilizers have been widelyused to control particle size, prevent the spontaneous agglomeration of nanoparticles and also functionalise the nanomaterials which make them suitable for their use in pharmaceutical and biomedical products [52-54]. Biopolymers would also be suitable as templates as they are biocompatible and biodegradable. Many successful examples of the use of polysaccharides for controlled synthesis of iron oxide nanoparticles can be found. Due to their low toxicity, magnetic iron oxides, such as magnetite (Fe_3O_4) and maghemite (γ-Fe_2O_3), have long beenrecognized as potential components in biomaterials for various biomedical applications [55-58].

Previous studies have shown that some polysaccharides havethe ability to interact with iron complexes, preventing theprecipitation of iron hydroxide and enabling nanoparticlesynthesis to occur under controlled conditions. For instance, several reports exist involving co-precipitation process in the presence of dextran [59-62]. Other biopolymers used include cyclodextrin [63], alginate [64, 65], chitosan [66], starch-based coatings [67, 68], and κ-carrageenan [69, 70]. Furthermore, studies alsohave been carried out on the interaction of κ-carrageenan withseveral transition-metal oxides and a structural model has been proposed for the biomineralization of iron oxides in the presence of this polysaccharide [71, 72].

κ-carrageenanhas thus been used as coating for magnetic particles has been suggested in order to induce the formation of a self-assembled nano reactor within which iron oxides nanoparticles are stabilized [73]. Encapsulation of magnetic nanoparticles in a polymeric matrix, such as polylactic acid (PLA) or polylactic-co-glycolic acid (PLGA) microspheres [74, 75] have been reported for use in targeted drug delivery system. Thermo responsive magnetic materials were obtained using some temperature-responsive polymers [76] such as poly (N-isopropylacrylamide), poly (NIPPAm), poly(ethylene oxide)-poly(propylene oxide)-poly(ethylene oxide)and so on. The disadvantage of this method was that many nanoparticles were encapsulated in polymeric matrix together, whichmade the nanoparticles agglomerate and limited the application in biomedicine. However, the polymer-encapsulated methods have somedrawbacks: (1) broad distributions of magnetic nanoparticles in size and shape are generally synthesized through this method, [77]; (2) functional magnetic nanoparticles with thismethod are unstablewhen the external environment is changeddue to lack of the strong chemical bonds between polymer and magnetic nanoparticles. Another method was to graftpolymer chains with some functional groups on the magnetite nanoparticle surface [78]

Magnetite nanoparticles, prepared by co-precipitation of Fe^{2+} and Fe^{3+} with NH_4OH, can be stabilized with silica to form well-dispersed magnetic silica nanospheres so that the hydroxyl surface groups can be chemically modified to afford different bioconjugation groups, such as amine and carboxylate. The size of the particles can be controlled by changing the SiO_2/Fe_3O_4ratio. Aminosilane has been covalently coupled to the surface of the magnetic silica nanoparticles and activated by glutaraldehyde to immobilize BSA.

Several researchers have studied the possibility of using alkanesulphonic and alkanephosphonic acid surfactants as efficient binding ligands on the surface of Fe_2O_3 nanoparticles andasstabilizers for particledispersioninorganic solvents [79, 80].

Iron oxide nanoparticles can be coated with silica, gold, or gadolinium (III) [81-90]. These coatings not only provide stability to the nanoparticles in solution but also help in binding various biological ligands to the nanoparticle surface. These nanoparticles have an inner iron oxide core with an outer metallic shell of inorganic materials. Silica has been exploited as a coating material for magnetic nanoparticles [91-97].

In the past decade, the synthesis of superparamagnetic nanoparticles have been of scientific interest due to their unique properties and being suitable for technological and medical applications [98-102,103-106].

The stabilization of the iron oxide particles is also crucial to obtain magnetic colloidal ferrofluids that are stable against aggregation in both a biological medium and a magnetic field [107-109].

Chitosan is an alkaline, nontoxic, hydrophilic, biocompatibleand biodegradable polymer. Nowadays, the preparations of magnetic nanoparticles encapsulated in chitosan are of great interest [110-111]. Kim et al. [112] have synthesized SPIO by a sonochemical method. Lee et al. [113] have prepared spherical SPIO nanoparticles about 15 nm in radius by sonochemistry and embedded them in chitosan to synthesize a ferrofluid.

Polymeric core/shell magneticnanoparticles could also be synthesized by using preformed synthetic polymers as a matrix to control the formation of magnetic cores [114,115].

In order to adopt a simple procedure for the synthesis of iron oxide nanoparticles to be applied in AOP for environmental remediation it was felt that an attempt could be made to adopt a simple, green, and aqueousco-precipitation method for the preparation of iron oxidenanoparticles stabilised with palm shell extract (IO). The IO could then be incorporated into chitosan to form a bionanocomposite CIO The objective of the present study was to evaluate thecharacteristics of IO and CIO by various spectroscopic techniques, magnetic properties by VSM and Mossbauer techniques and also investigate the effectiveness of IO and CIO as fenton's reagents (H_2O_2/Fentons) in degrading the textile dyes RB-21,RR-141 and Rh- 6G and the binary mixture of dyes (RB+RR), (RR+RH) and (RB+RH).

3.2. Materials and Methods

3.2.1. Synthesis of Palm shell extract, Ironoxide (IO) and Chitosan/ ironoxidenanocomposite (CIO)

Synthesis of Palm Shell Extract Capped Iron oxide nanoparticles (IO)

The palm shell extract used for capping iron oxide particles was prepared as mentioned in Chapter 2 section 2.12. The iron oxide nanoparticles were synthesised by co-precipitation of Fe^{3+} and Fe^{2+} salts in the ratio 2:1 in the presence of aqueous Palm shell extract. 1 ml of 0.1N

NaOH was added to the above solution and kept in stirring for 2-3 mins. The colour of the solution changed immediately from brown to black indicating the formation of ironoxide nanoparticles. The nanoparticles were then washed with deionized water and dried at room temperature.

Synthesis of Chitosan -Iron oxide nanocomposite (CIO)

1% Chitosan solution in glacial acetic acid was added to the synthesised iron oxide nanoparticle solution in stirring condition for 60 mins. Dark brown coloured solution of the nanocomposite was formed which was then poured into a Teflon plate and kept for drying at room temperature.

3.2.2. Individual and Binary dye degradation experiments

The respective individualsolutions [Reactive blue -21 (RB-21), Reactive red – 141 (RR-141) and Rhodamine 6G (Rh-6G) and binary mixture of dye solutions(RB+RR, RR+RH,RB+RH) prepared by dissolving the required amount of dye in 100 mL of DDW. Samples were prepared by mixing 3 mL of the dye solution, 0.5 mg catalyst and 200 μL of 30% H_2O_2 in a cuvette. The cuvette was then inserted in the spectrophotometer, Scans were started immediately after the addition of nanoparticles, and the solution was left untouched until completion. Absorbance was monitored at the respective maximum wavelength.

3.2.3 Characterisation

The dried IO as well as CIO were characterised by FTIR, XRD, Raman, SEM EDS, TEM and X-Ray Photoelectron Spectroscopy (XPS) techniques. XPS analysis was done using KRATOS AXIS Ultra HAS instrument. The nanoparticles were further characterised by Vibrating Sample magnetometer (model no 7400) with P.S-665. Mossbauer spectroscopy was recorded in transmission geometry using constant acceleration drive (CMTE-250) with a 5mCi 57Co in Rh matrix at room temperature. The mossbauer spectra of Fe was used as reference.

The same instruments and methodologies were adopted for characterisation using FTIR, XRD, Raman, SEM EDS, TEM techniques as discussed in chapter 2.

3.3 Results and Discussion

3.3.1 Zeta potential measurements

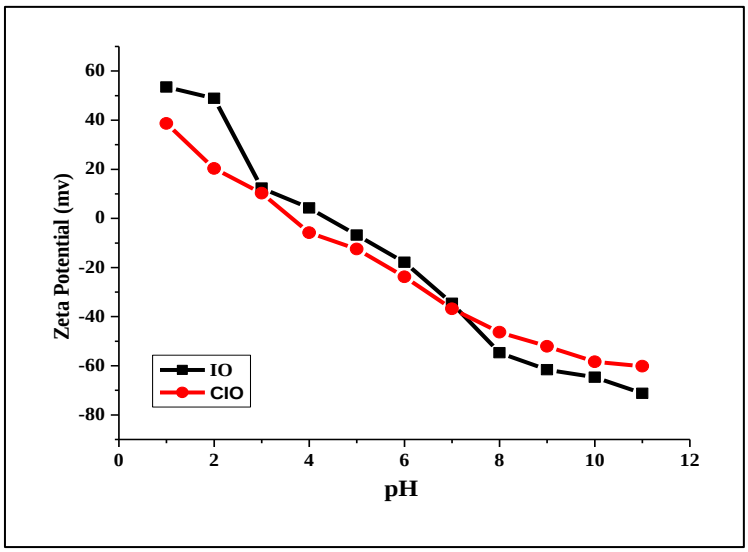

Figure 3.1 Zeta potential of IO and CIO

Figure 3.1 shows the zeta potential of IO and CIO as a function of pH. It showed that the zeta potential of IO and CIOwas positive at lower pH and negative at higher pH.

3.3.2 FTIR spectroscopy

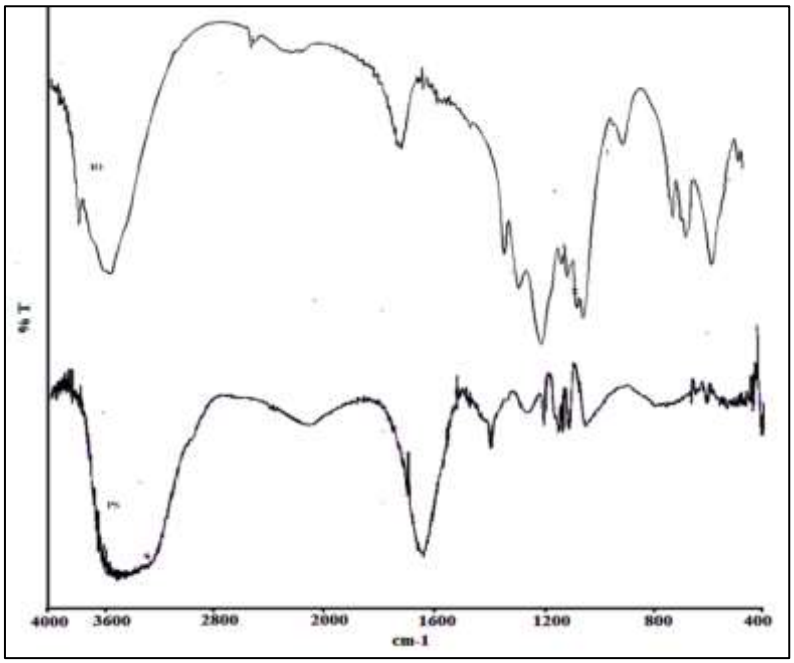

Figure 3.2 IR spectra of Palm shell extract and iron oxide

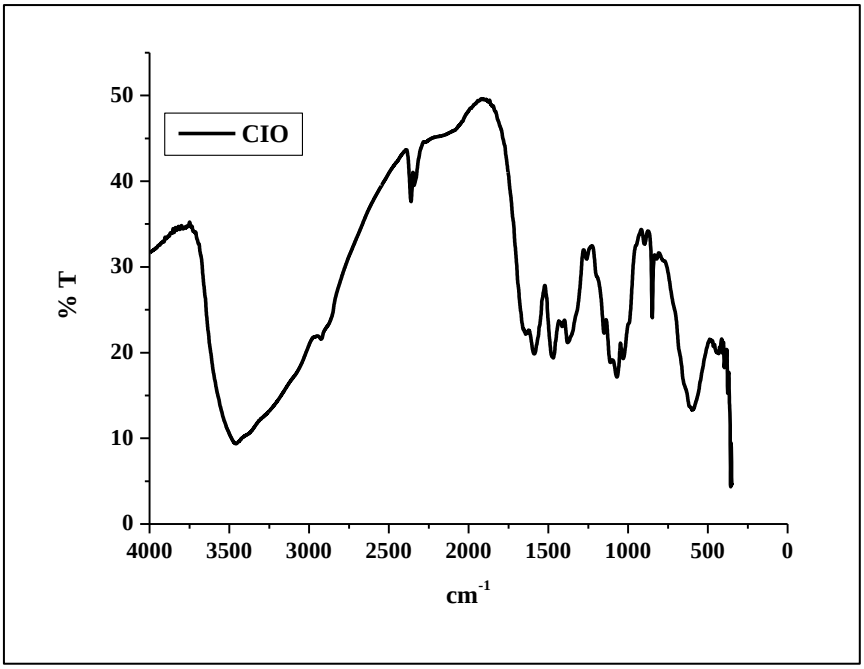

Figure 3. 3 IR spectra of Chitosan-iron oxide nanocomposite

Figure 3.2shows the spectrum recorded for the palm shell extract (PS), iron oxide IO) and Figure 3.3 shows the IR spectra of Chitosan-ironoxide nanocomposite (CIO). The peak at 1556 $cm^{-1}$and 1634 cm^{-1}in iron oxide nanoparticle corresponds to the amide I and II bands of proteins, respectively. The band at 1634 cm^{-1}can be assigned to the carbonyl groups present in the extract. The peaks at 665, 608 cm^{-1} correspond to Fe-O stretching vibrations. The bands between 400 $cm^{-1}$and 800 cm^{-1}in the IR spectrum of the palm shell extract can be attributed to bending vibrations of C-H bond deformations in acetylenic groups, aliphatic CH_3 deformation and rocking modes, NH_2 and N–H wagging modes of amines and olefinic cis-CH= CH, and the out-of plane bending vibrations of the alcoholic and phenolic O–H bonds. The strong bands appearing in the FTIR spectrum of the extract between 1000 cm^{-1} and 1260 cm^{-1} is within the range of strong C–O vibrations of carboxylic acids, alcohols and phenols and medium-to-strong C–N vibrations of amines and amides. The peak at 1383 cm^{-1}in the case of iron oxide and palmshell extract can be attributed to aliphatic CH_2 and CH_3 groups, CH_2 groups of aldehydes and ketones, bending modes of O–H bonds in alcohols and phenols and carboxylic acids. This indicates that the synthesized iron oxide nanoparticles are stabilized by polysaccharides, proteins and phenols (116-119). The IR band at 3457cm^{-1} in the case of CIO can be assigned to the stretching modes of surface H_2O moleculesor to an

envelope of hydrogen-bonded surface OH groups.The bands at 665cm^{-1} can be attributed to Fe-O stretching vibrations. The peak at 1570 cm^{-1} and 1469cm^{-1} are attributed to amide I and amide II bands of chitosan. The peaks at 1360 cm^{-1} and 1070 cm^{-1} are the stretching vibrations of -CH_3 and –C-O-C of chitosan. The band at 1634 cm^{-1} in IO is shifted to 1570 cm^{-1}in CIO indicating the formation of hydrogen bonds between chitosan and the palm shell extract as also corroborated by the shift in amide bands [120]. The peak at 597 cm^{-1}in CIO corresponds for the Fe-O stretching vibrations which implies the formation of the nanocomposite [121].

3.3.3. X-ray diffraction method

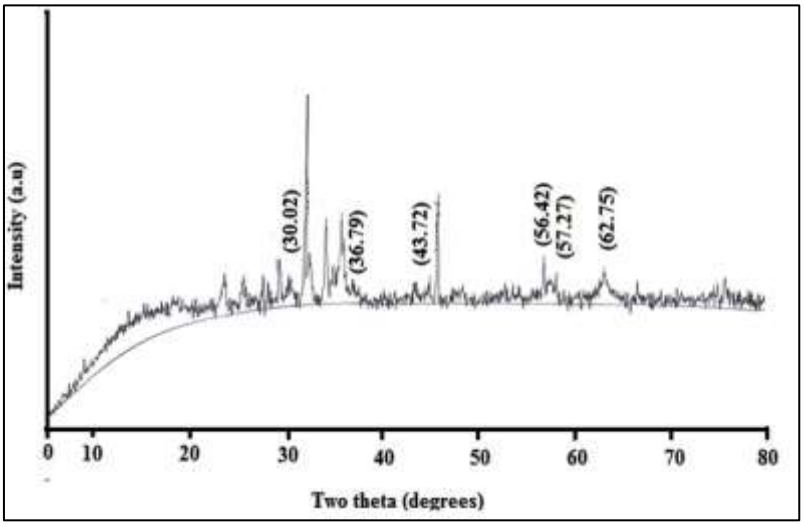

Figure 3.4 X-ray diffraction pattern of Iron oxide (IO)

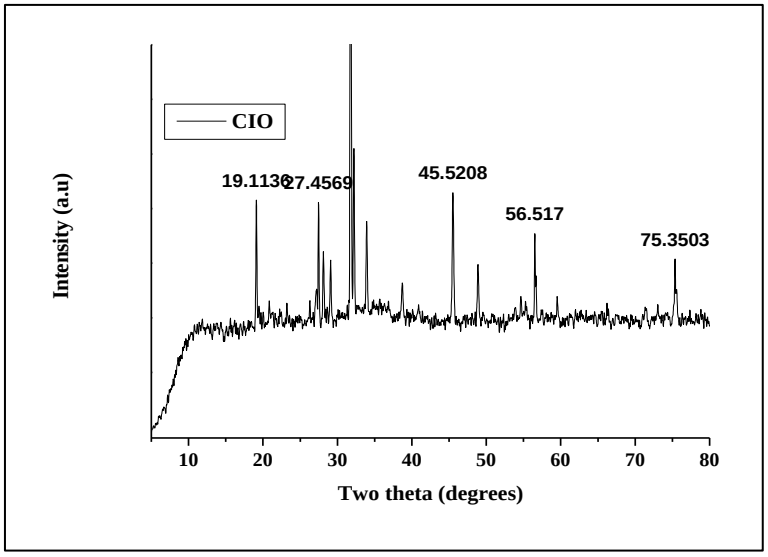

Figure 3.5 X-ray diffraction pattern of Chitosan-Iron oxide (CIO)

Figure 3.4 and 3.5 shows the X-ray diffraction pattern of Iron oxide nanoparticle (IO) and Chitosan iron oxide nanocomposite (CIO). The XRD spectra give a clearcrystalline pattern attributable to Fe_3O_4 nanoparticles in both samples[122]. The 2θ peaks at 30.02A^0, 36.79 A^0, 43.72 A^0, 56.42 A^0, 57.27 A^0 and 62.75 A^0 are attributed to the crystal planes of iron oxide at 220, 311, 222, 400, 422 and 511 respectively. The diffraction peaks are sharp and intense indicating the crystalline nature with cubic spinel structure of IO. CIO nanocomposite also shows similar peaks to Iron oxide nanoparticle with 2θ values at 27.45A^0, 38.71 A^0, 45.52 A^0, 56.51 A^0, 59.537 but with a slight shift in the 2θ values indicating the presence of iron oxide in the nanocomposite [123] and that the structure of iron oxide nanoparticles is not changed during incorporation into chitosan matrix.The nanocrystalline spinel could be due to either Fe_3O_4 or γ-Fe_2O_3. Further some weak peaks (~25,~35,~39) due to hematite (α-Fe_2O_3) werealso detected in IO and CIO. Thus, since thelattice parameters of oxides have very little differences and moreover, due to their nanophase existence their XRD identification is difficult [124]. The average diameter of synthesized iron oxide nanoparticles was determined to be 36 nm using the scherrer equation (Chapter 2, section 2.25). The crystallites present are small enough to display superparamagnetic properties. The colour of IO observed was Blackish and the nanocomposite was brownish which indicates the predominance of different phasesin IO and CIO.

3.3.3 Raman spectroscopy

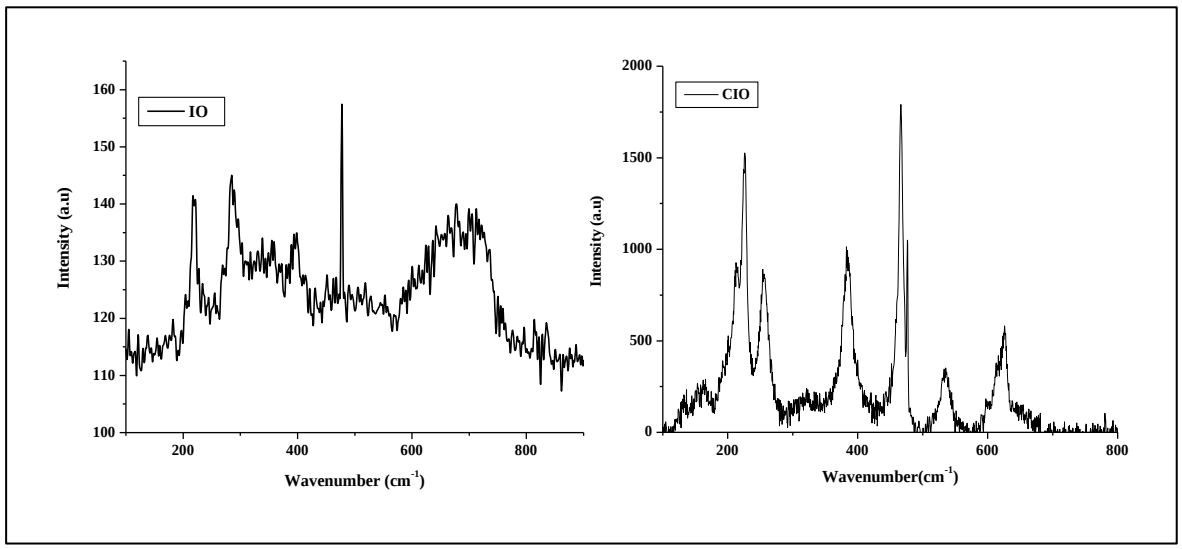

Figure 3.6 Raman spectraof IO and CIO

Figure 3.6 shows the Raman spectra of IO and CIO. In the case of IO the peak at 217 cm^{-1} is due to Fe–O symmetricstretching in haematite phase while in CIO it is at 227 cm^{-1}. Also the peaks at 284 and 398 cm^{-1}may be due to the Fe-O asymmetric bend of magnetite. The peak at 477 cm^{-1}might be due to Fe-O asymmetric bend of maghemite. The peak at 677 and 518$cm^{-1}$is due to Fe-O symmetric stretching of magnetite in IO and at 537cm^{-1}in CIO [125]. The presenceof these peaks suggestthat the synthesised IO is a mixture of different phases. The presence of Raman peaks in the region of 200-400 cm^{-1} suggests α-Fe2O3 phase in IO and CIO. This suggests the possibility of all the three phases in IO and α- Fe2O3 in CIO.

3.3.4. Transmission electron Microscopy

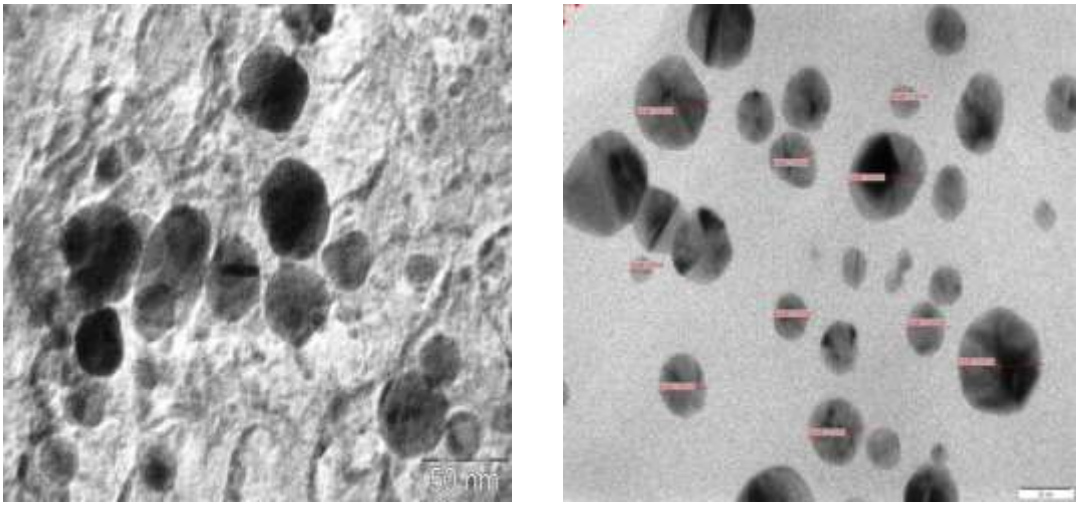

a) IO **b) CIO**

Figure 3.7 TEM images of a) IO b) CIO

Figure 3.7 shows the TEM micrographs of iron oxide nanoparticles (IO) and the Chitosan-iron oxide nanocomposite (CIO) which clearly suggest that there is formation of hexagonal to distorted hexagonal shaped particles in IO while in CIO the shape of the particles have become uniformly hexagonal. The palm shell capped IO nanoparticles are seen to have an average size of 50 nm while CIO is seen to have an average particle size of 20 nm. However there are particles of very small size ranging from 9-11 nm in IO and CIO. These small sized particles are more in CIO. Furthermore, the particles in IO and CIO seem to have tendency to form chains.

3.3.5 Energy dispersive X-ray analysis

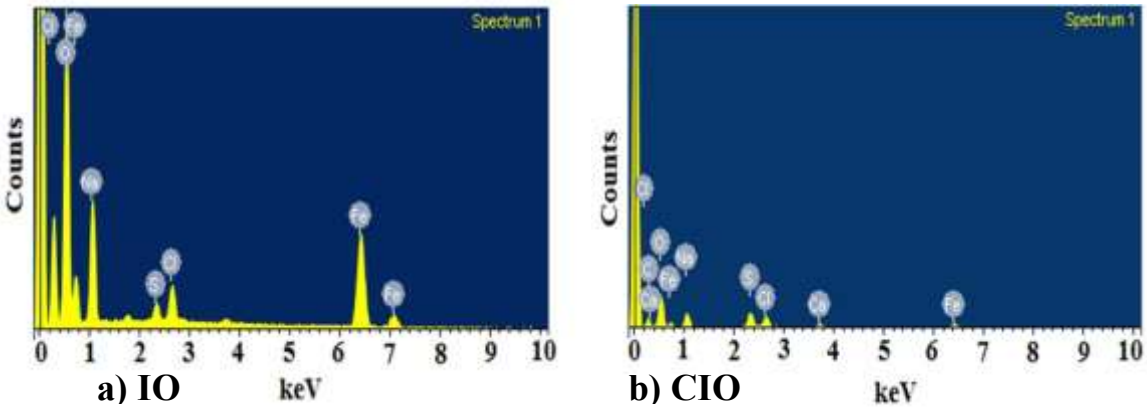

Figure 3.8 EDAX images of a) IO b) CIO

The Energy Dispersive X-ray (EDX) analysis showed in Figure 3.8 confirms thepresence of iron and oxygen elements in IO and CIO. The presence of other metals like Na and Ca indicates that the nanoparticles are stabilized using palmshell extract.

3.3.6 Vibrating sample magnetometer analysis

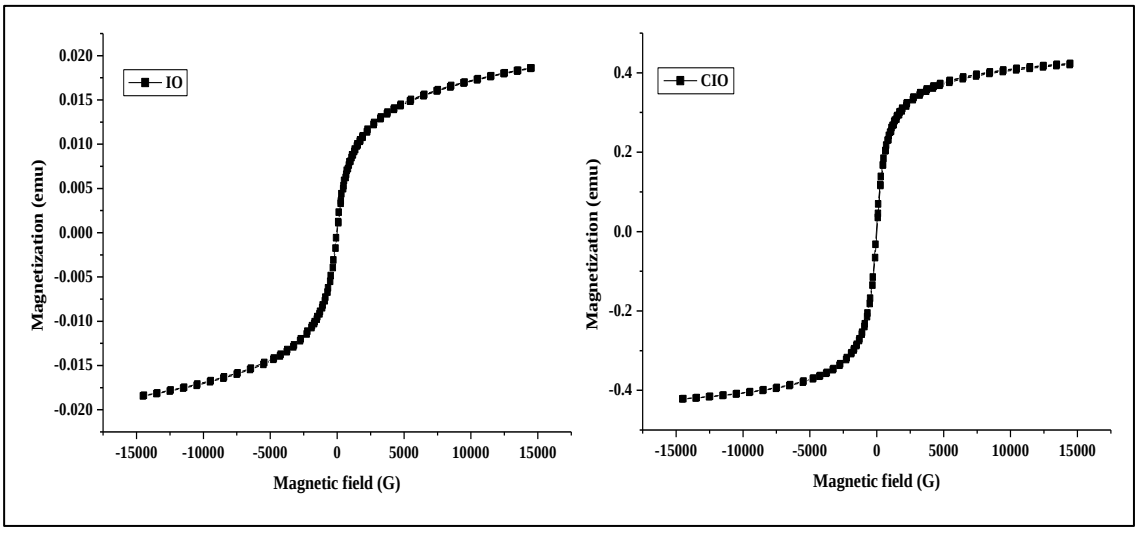

Figure 3.9 VSM spectra of a) IO b) CIO

The magnetic properties of the synthesised iron oxide nanoparticles were studied using a vibrating sample magnetometer (VSM). A magnetic field was applied to a powdered sample and the magnetization response was investigated. The magnetic property of iron oxide nanoparticles and chitosan iron oxide nanocomposite was obtained by field dependent magnetization measurements. The saturated magnetization value for the iron oxide nanoparticles and Chitosan iron oxide nanocomposite is found to be 0.018 emu /mg and 0.420 emu /mg. The saturation

magnetization increased after coating with chitosan and is equivalent to superparamagnetic iron oxide nano particles (SPIONS), as there are a greater number of particles with sizes capable of exhibiting superparamagnetic properties. The difference in magnetization valuebetween IO and CIO can be attributed to the further encapsulation of nonmagnetic chitosan component [126]. The absence of hysteresis loop and coercivity further affirms the superparamagnetic nature of the iron oxide nanoparticles in IO and CIO. The reason for thesuper-paramagnetism of IO and CIO is mainly that the size of some of the nanoparticles is so small thateach particle can be considered to be equivalent to a single magnetic domain and the energy barrier for its spin reversal is easily overcome by thermal vibrations [127].

3.3.7 X-ray photoelectron spectroscopy

Figure 3.10 (a, b, c, d) and 3.11 (a, b, c, d) shows the xps spectra of IO and CIO. Table 3.1 shows the binding energy values of IO and CIO.

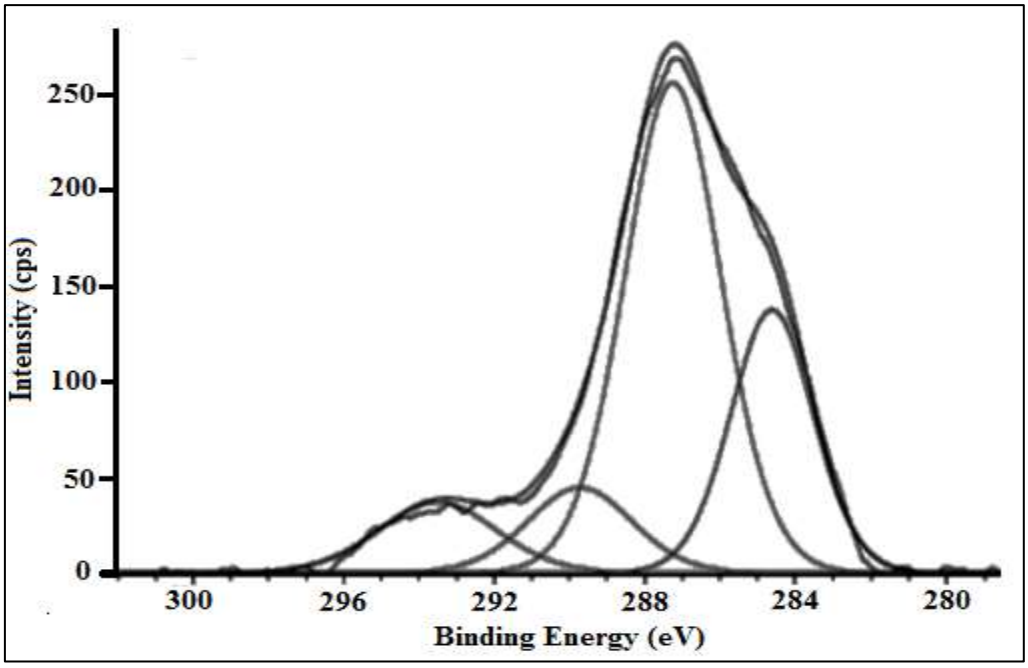

Figure 3.10 a) XPS (C1S) spectra of IO

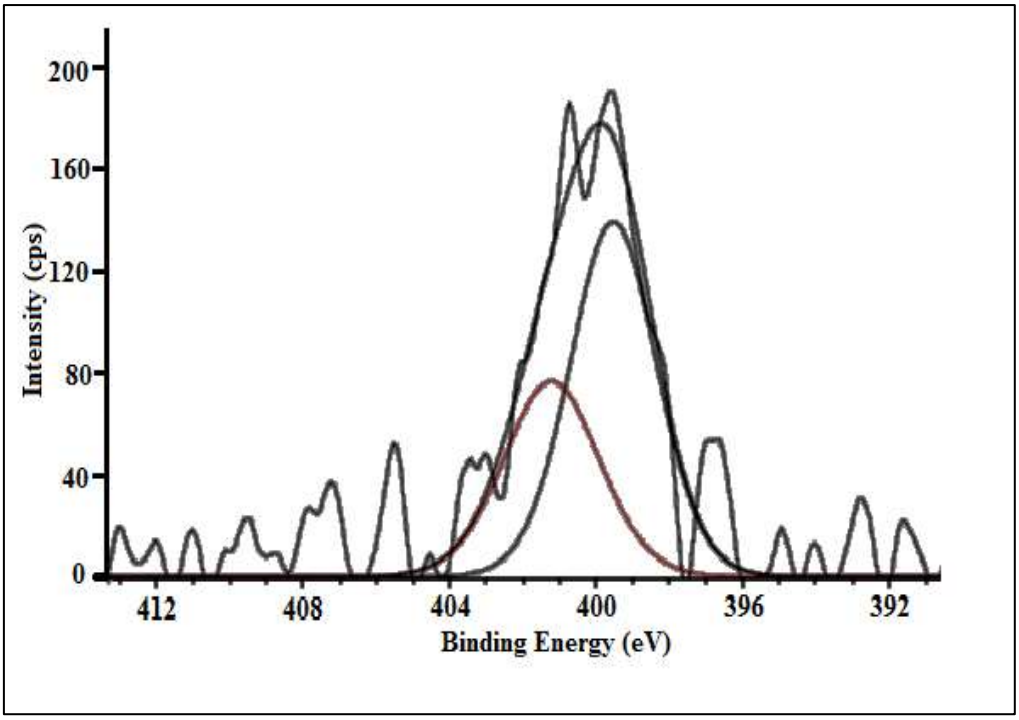

Figure 3.10 b) XPS (N1S) spectra of IO

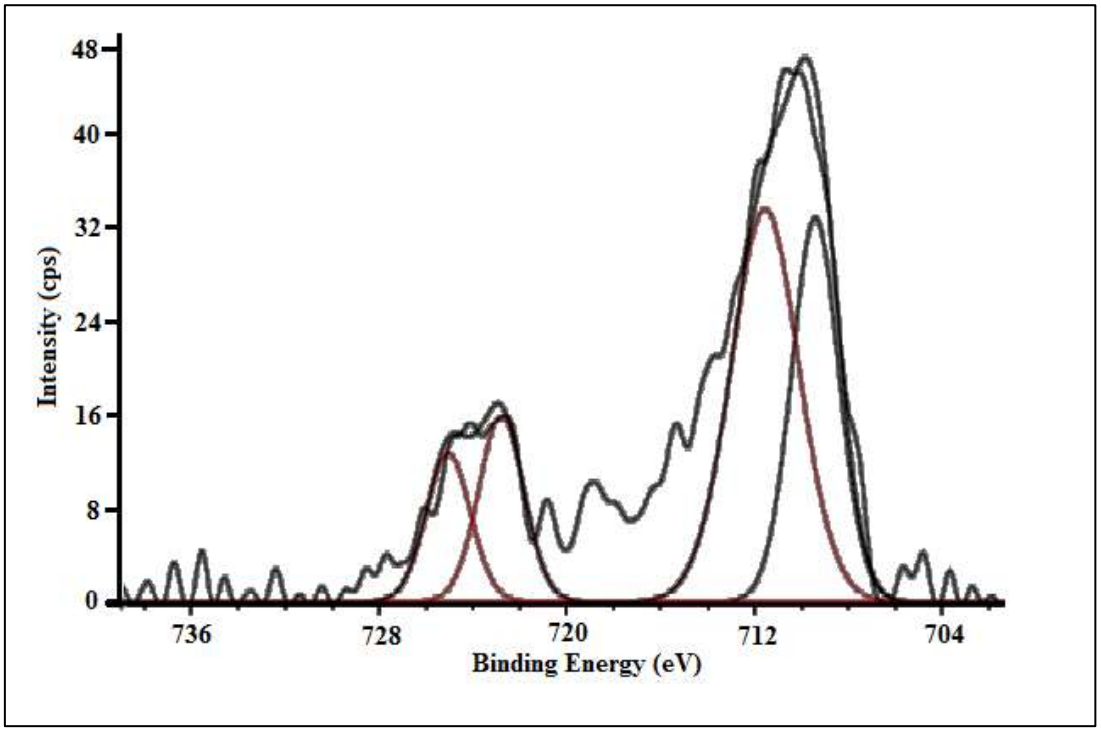

Figure 3.10 c) XPS (Fe 2p) spectra of IO

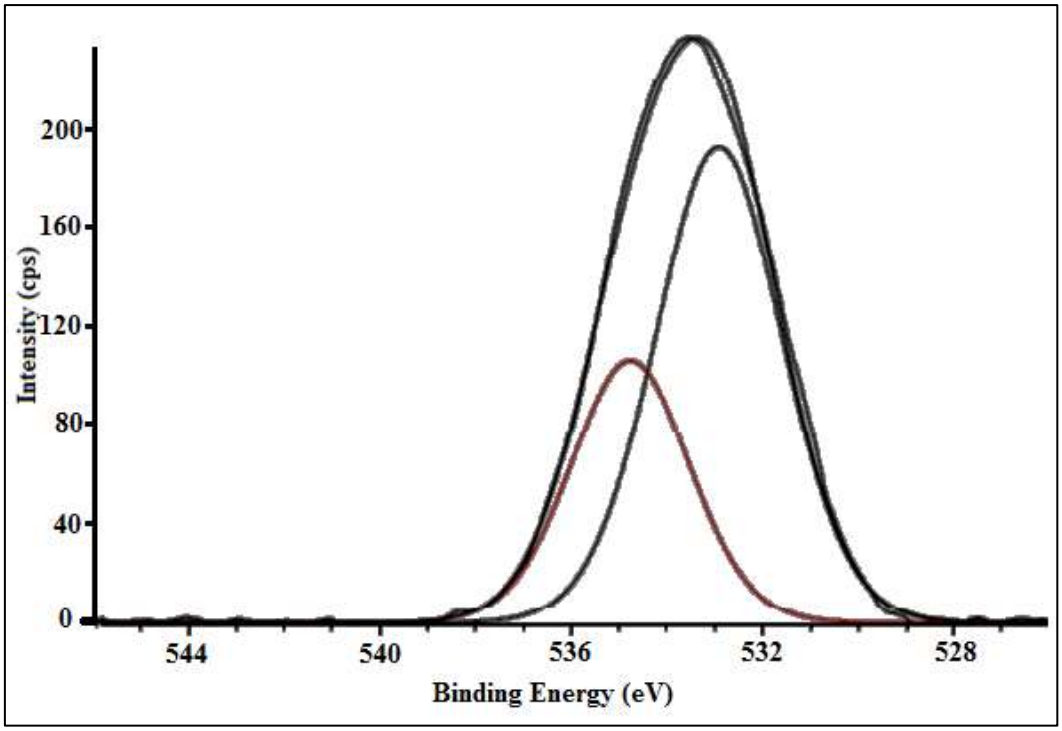

Figure 3.10 d) XPS (O1S) spectra of IO

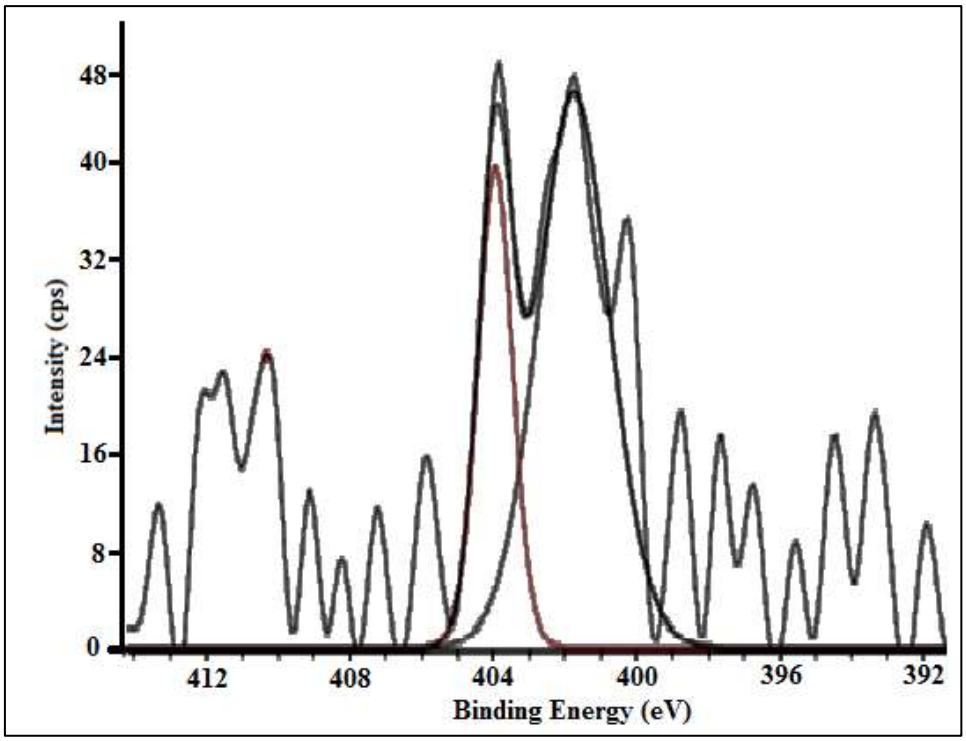

Figure 3.11 a) XPS (N1S) spectra of CIO

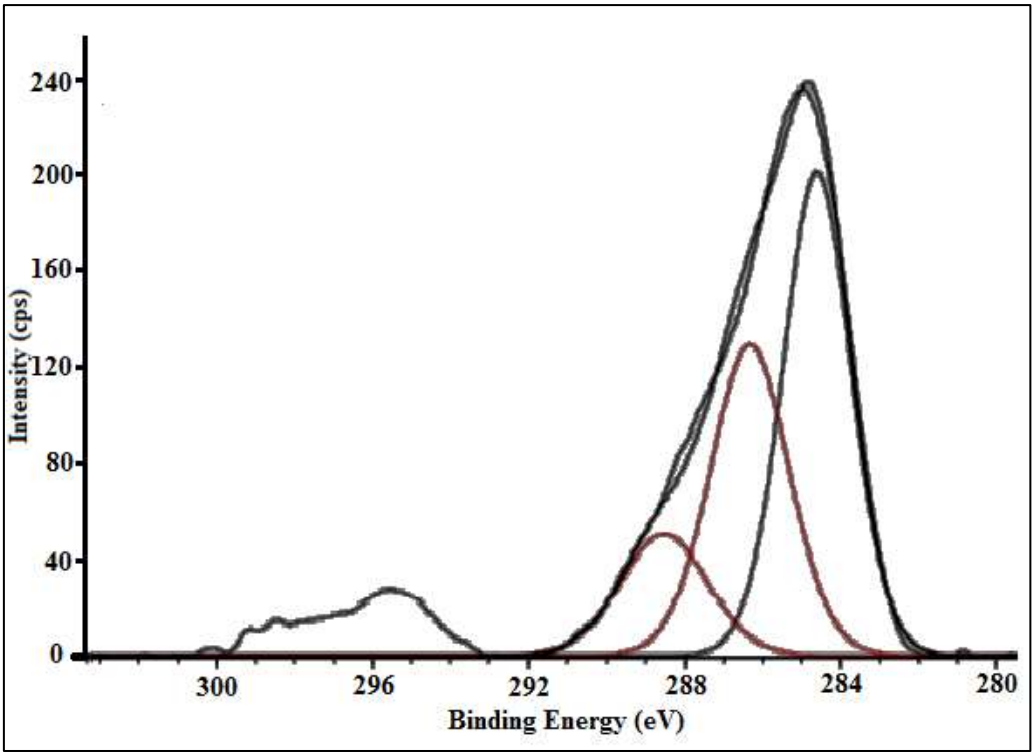

Figure 3.11 b) XPS (C1S) spectra of CIO

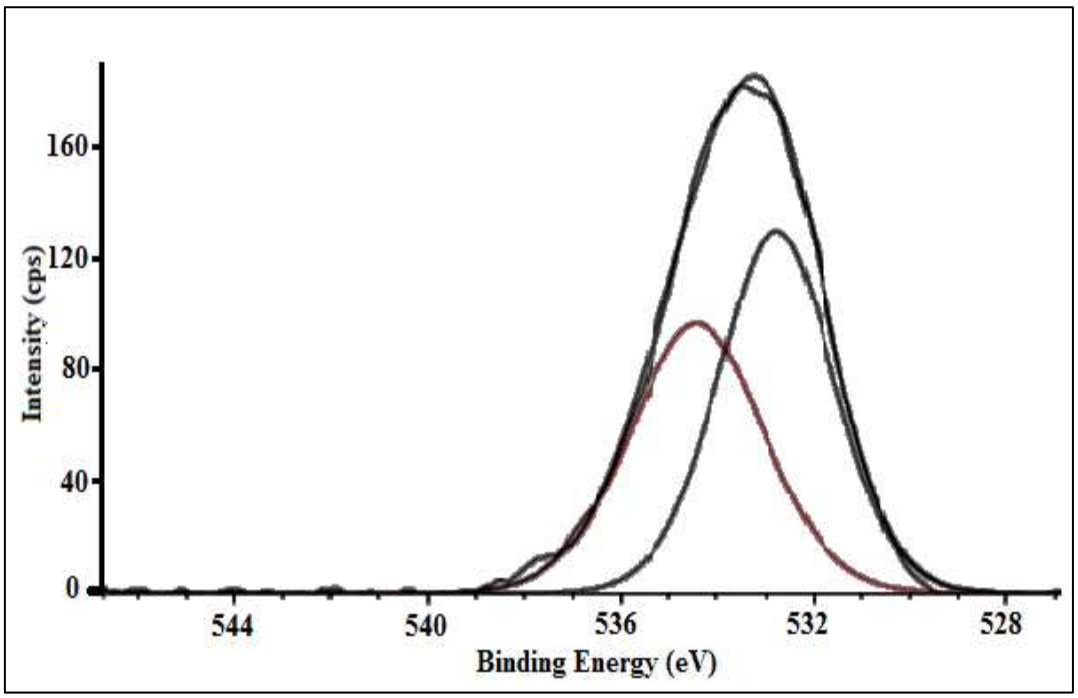

Figure 3.11 c) XPS (O 1s) spectra of C IO

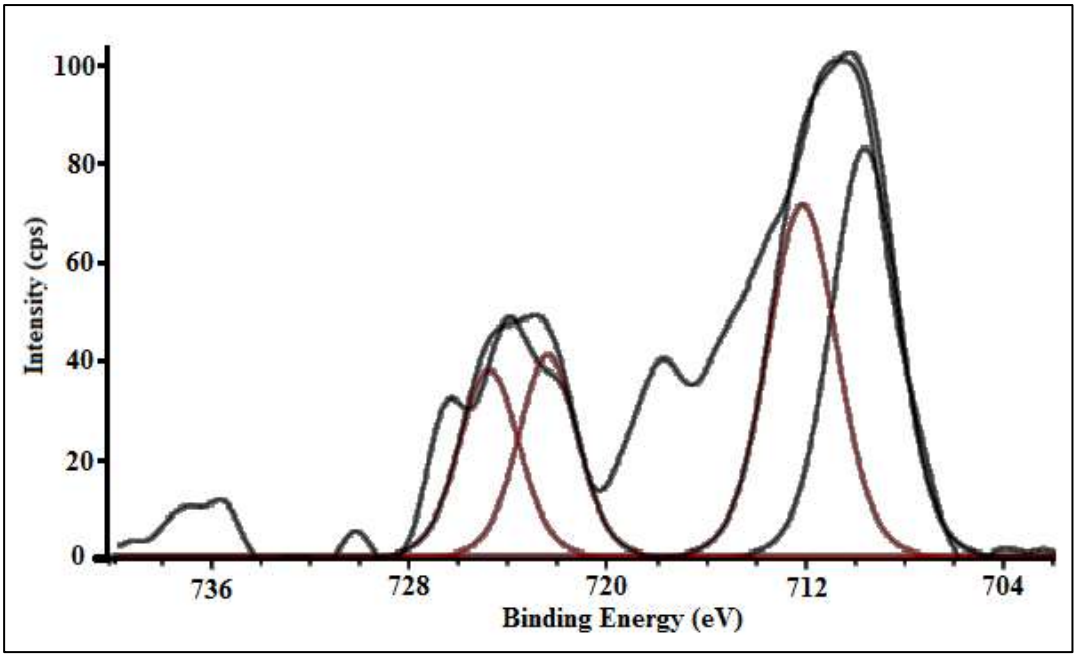

Figure 3.11 d) XPS (Fe 1s) spectra of CIO

Table 3.1 Binding energy of IO and CIO

	Binding Energy (eV)	**FWHM**	**Area**	**%**
IO				
C1s	284.667	2.546	9945.2	25.2
C1s	287.286	2.978	21677	54.8
C1s	289.724	3.233	4084.6	10.3
C1s	293.531	3.638	3815.3	9.7
N1s	399.532	2.73	1265.4	62.1
N1s	401.256	3.021	771.7	37.9
Fe2p	709.41	2.335	1412.8	30.3
Fe2p	711.562	3.352	2072.9	44.5
Fe2p	722.808	2.243	658.7	14.1
Fe2p	725.091	2.201	517.3	11.1
O1s	532.925	3.071	256125.5	65.9
O1s	534.794	2.871	13242.8	34.1
CIO				
C1s	284.642	2.011	11719.7	48.3
C1s	286.33	2.335	8741.1	36
C1s	288.532	2.608	3807.4	15.7
N1s	401.75	2.329	371.6	70.7
N1s	403.95	1.111	154	29.3
O1s	532.81	2.734	11978.4	53.8
O1s	534.427	3.163	10281.5	46.2
Fe2p	709.633	3.121	435.5	36.7
Fe2p	722.425	2.759	188.9	15.9
Fe2p	712.72	3.211	385.2	32.4
Fe2p	724.825	2.794	178	15

The N binding energy of ~ 401.7 ev in IO and CIO can be attributed to amide nitrogen of protein from palm shell extract. The N 1s binding energy at ~ 399.5 eV in IO can be assigned to NH-C(O) while the peak at 403.9 eV in CIO was assigned to Fe-NH_2 bond [128] suggesting that Fe is bound to proteins and chitosan. The binding energy of O(1s) at 532.925 eV in IO and 532.810 in CIO may be attributed to oxygen atoms binding withorganic elements [129]. The component at 532.9 eV is wider with a FWHM of 3.0eV. This component could be attributed to OH and furthermore the high FWHM value suggests that the peak may also include an additional unresolved component, such as adsorbed oxygen O^- or O_2^{2-} observed typically at about 0.7 and 2 eV higher than the lattice oxygen, respectively [130]. The peak with binding energy~ 534 eV in IO and CIO could be attributed to oxygen singly bonded to carbon such as carboxyl groups of the palm shell extract. The major peaks at 709.4 (Fe^{2+}IO), 711.5(Fe^{3+}IO); 709.6(Fe^{2+}CIO); 712.1eV (Fe^{3+}CIO) and 725.091eV (Fe^{3+}IO), 722.8eV (Fe^{2+}IO); 722.4eV (Fe^{2+}CIO), 724.825 eV (Fe^{3+}CIO) to the $2p_{3/2}$ and $2p_{1/2}$ core levels of iron oxide respectively. The presence of two peaks for $2p_{3/2}$ and $2p_{1/2}$ levels could be attributed to the presence of two different types of iron (Fe^{2+} and Fe^{3+}) in iron oxide particles suggesting the presence of magnetite. Similar results were reported by Chowdhury et al [131]. Furthermore it is seen that, the peak full width at half maximum (FWHM) was found to be between 2.2 and 3.3 eV. According to Hochella [132] 2p sublevels of transition metals in high-spin or paramagnetic states exhibit considerable line broadening due to complex multiplet splitting phenomena. The satellite peaks at 729 eV in IO and 730 eV in CIO, can be attributed to Fe $2p_{1/2}$ of γ-Fe_2O_3, which though weak can be differentiated from Fe_3O_4. Theshoulder peak between Fe $2p_{3/2}$ and Fe $2p_{1/2}$ further confirms the presence of γ-Fe_2O_3 phase.

3.3.8 Mossbauer spectroscopy analysis

Figure 3.12a and 3.12 b shows the Mossbauer spectra of IO and CIO. The Mossbauer spectra for CIO were of complex nature and consisted of two magnetic sextets and a singlet for IO while mossbauer spectra of CIO displayed two singlets. The sextets in IO could be assigned to α-Fe while the singlet could be assigned to magnetite/maghemite of small particle size. Nedkove et al [133] as well as Morup et al [134] have reported the presence of a superparamagnetic singlet in the mossbauer spectrum at 227 K of magnetite with particle size of 6 nm.

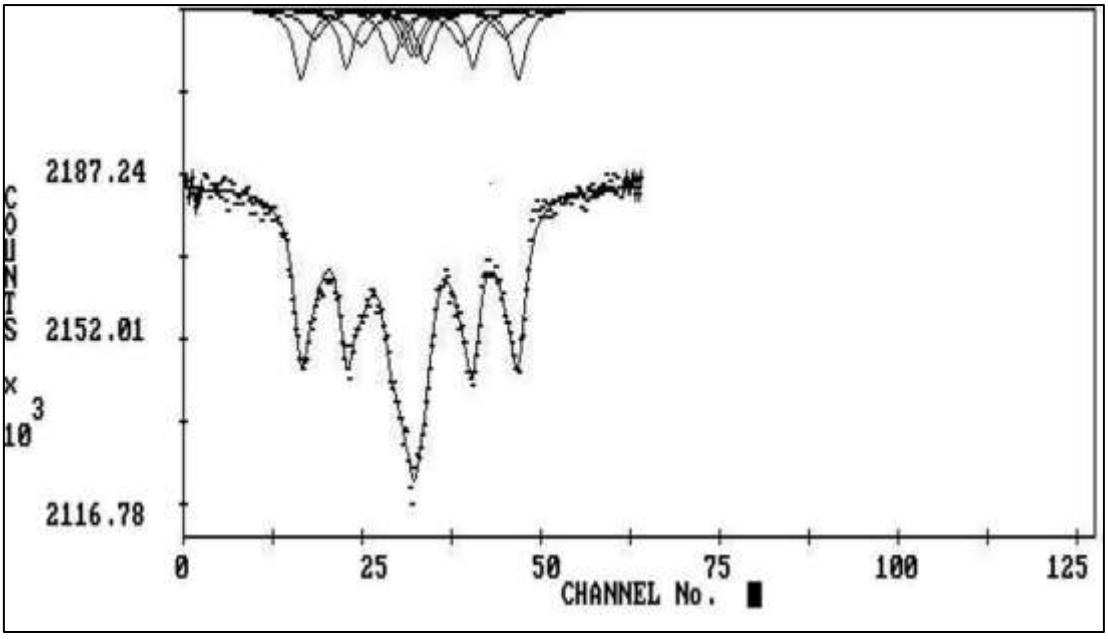

Figure 3.12 a) Mossbauer spectra of IO

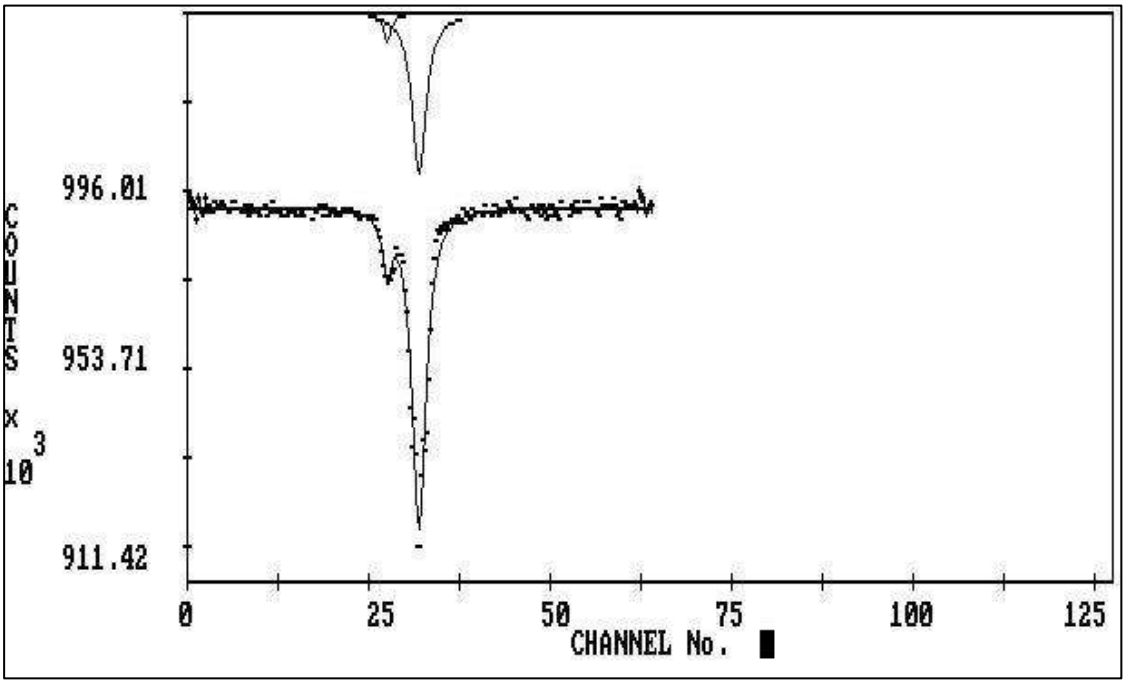

Figure 3.12 b) Mossbauer spectra of CIO

Furthermore, materials like magnetite and maghemite crystallize in regular structure; therefore, superparamagnetic relaxation is observed in the form of a singlet rather than a doublet [135]. Table 3.2 shows the Mossbauer parameters.

Table 3.2 Mossbauer data parameters

		Isomer Shift	**Fractional area**	**Field**
Calib spectrum		Velocity calibration = 0.121mm/sec Resolution : 0.59mm/sec		
IO	Singlet	-0.85	0.05	
	Magnetic	-0.40	0.53	456.6 (0.05)
	Magnetic	-0.24	0.42	401.9(0.05)
CIO	Singlet	-2.37(0.02)	0.10	----
	Singlet	-0.24	0.9	-----

A broad weak singlet in CIO suggests another paramagnetic contribution (around10%) with anomalous large values of isomer shift. However, broad single line shape is also characteristic for superparamagnetic state of iron magnetic moments.Lackof the sextet in the case of chitosan is probably attributed to smaller diameters of nanoparticles in those systems. The diameters of the nanoparticles (affirmed by TEM, XRD) are small enough to show such behaviour. One singlet in IO and two singlets in CIO could be attributed to superparamagnetic iron oxide nanoparticles (SPIONS) of different sizes and number. However some particles are big enough in IO to give rise to a sextet. The subspectral areas and magnetic hyperfine field donot indicate the presence of pure single phase Fe_3O_4.The hyperfine fieldsplitting of the sextuplet, 456kOe and 409 KOe are quite low as compared with the value of515 kOe for bulk α-Fe_2O_3. This indicates the presence of small bimodalα-Fe_2O_3 particles (diameter between 7 and 12 nm) in IO.Further, as the hyperfine field of α-Fe_2O_3 is same as that ofγ-Fe_2O_3, the mossbauer lines of these phases overlap and the possibility of the presence of all these phases exist. The contribution from α-Fe_2O_3 must also be considered as the presence of this phase is observed in the XRD pattern and Raman spectra. Hence, the observed Mossbauer spectrum is acontribution from Fe_3O_4, γ-Fe_2O_3 and α-Fe_2O_3in IO and CIO with predominance of SPIONS in CIO. The anomalous high negative isomer shift in CIO could not be accounted for. It could be due to the increased tendency of the iron oxide particles to form chains and hence interaction between these particles.

Though iron-57 isomer shift is a useful technique for characterizing the oxidation states, it can be seen from the table that an anomalously large negative isomer shift of -2.37 is obtained for one singlet in CIO. The isomer shift is known [136, 137] to decrease as the s-electron density at the iron-57 nucleus increases. An increase in the electron density at the Fe nucleus could be due to an increased 4s-orbital population, or due to deshielding of 3s and 4s electrons by a decrease in the population of 3d-orbitals. The latter factor plays a more important role on the very negative isomer shifts of high oxidation state compounds such as the iron (VI) oxides [138].

However, such high oxidation states cannot be expected in IO and CIO. Gary long et al have reported in their Mossbauer study on Zr_6Cl1_4Fe, $LiZr_6Cl_{15}Fe$, and $KZr_6Cl_{15}F$ cage compounds large negative isomer shifts which they have attributed to electropositive environment felt by the iron atom within a Zr_6 cage [139]. It is probable that chitosan and palm shell extract together could provide a highly electropositive environment into which iron oxide is encapsulated resulting in large negative isomer shifts. The negative isomer shift obtained is highest reported to our knowledge. Such isomer shifts have not been reported for chitosan complexes of iron [140, 141, 142, 143,and 144].

The present observation can be attributed to interaction between chitosan and palm shell extract. However further work needs to be done to understand the mechanism. Raman, XPS, XRD and Mossbauer techniques suggest the presence of Fe_3O_4, γ-Fe_2O_3 and α-Fe_2O_3 in IO and CIO though to different extents. However the colour of IO particles were black suggesting magnetite was the major component as evidenced by Raman and Mossbauer. The CIO particles were reddish brown suggesting the predominance of α and γ Fe_2O_3.

3.3.10 Degradation experiments.

The degradation of individual (RB-21, RR-141 and Rh-6G) and mixture of dyes (RB+RR, RB +RH and RR+RH) was studied using IO and CIO as catalysts in the presence of H_2O_2at pH 6 under ambient conditions. Fig 2.11, 2.12, 2.13 and 2.14 show the UV spectra for degradation of individual and mixture of dyes.It was observed that individual dyes degraded within few minutes by handshaking of the dyes. In the case of mixture of dyes, using IO as a catalyst (RB+RH) binary mixture degradation was not complete (72%) even after 24 h, where it took only 2 min when

CIO was used as catalyst. On the other hand, complete degradation of RR+RH binary mixture took around 120 min and 35 min using IOand CIO as catalysts respectively while RB+RR degraded within 5 min when IO was used as catalyst and 35 min using CIO as catalyst. Blank experiments were also done to check the catalytic activity of only H_2O_2 in the absence of nanocomposite and it was observed that H_2O_2 does not play any role in the degradation of dyes. It is the high catalytic activity of the hybrid heterogeneous catalyst which has produced remarkable efficiency in degradation of dyes. The colourless solution after degradation was analysed for TOC to see the extent of degradation. The TOC value after degradation shows a decrease which indicates that mineralization has taken place. However CIO was able to mineralise Rh6G only to an extent of 12% though decolorisation took place suggesting that it was not effective in degradation of Rh6G. However in the binary mixture of RB+ RH TOC was reduced by 55% again affirming the fact that RB 21 may be playing a catalytic role in the degradation of Rh6G.

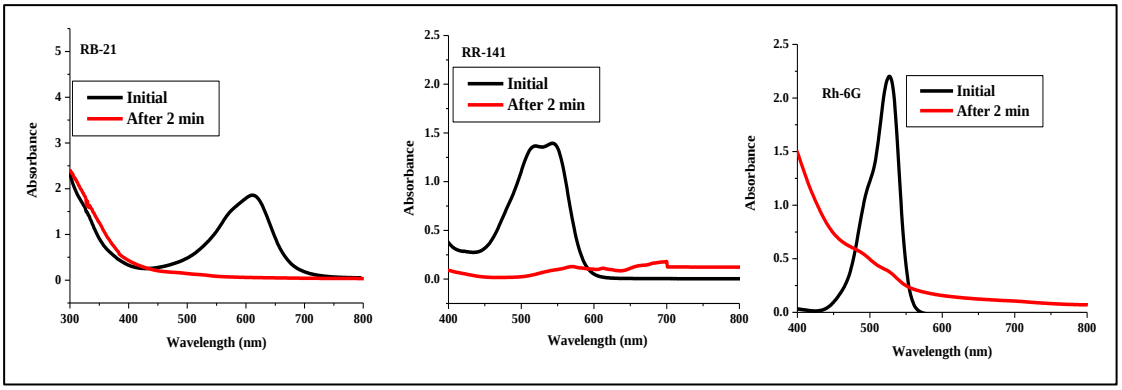

Figure 3.11 UV spectra for degradation of individual dyes using IO as a catalyst

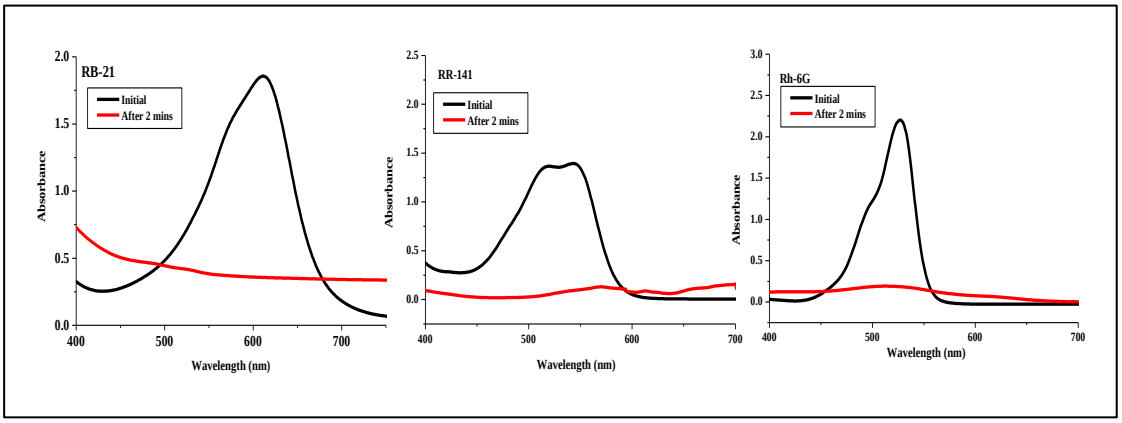

Figure 3.12 UV spectra for degradation of individual dyes using CIO as a catalyst

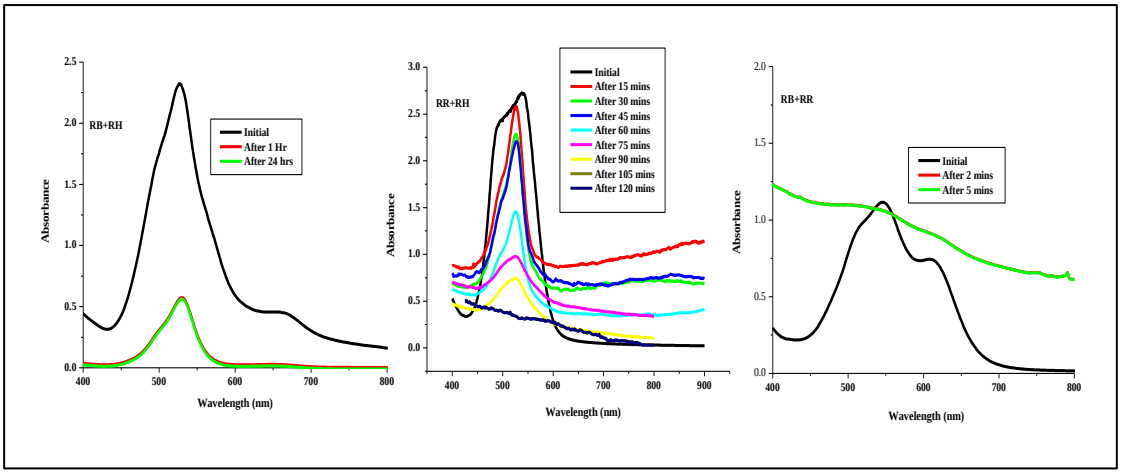

Figure 3.13 UV spectra for degradation of mixture of dyes using IO as a catalyst

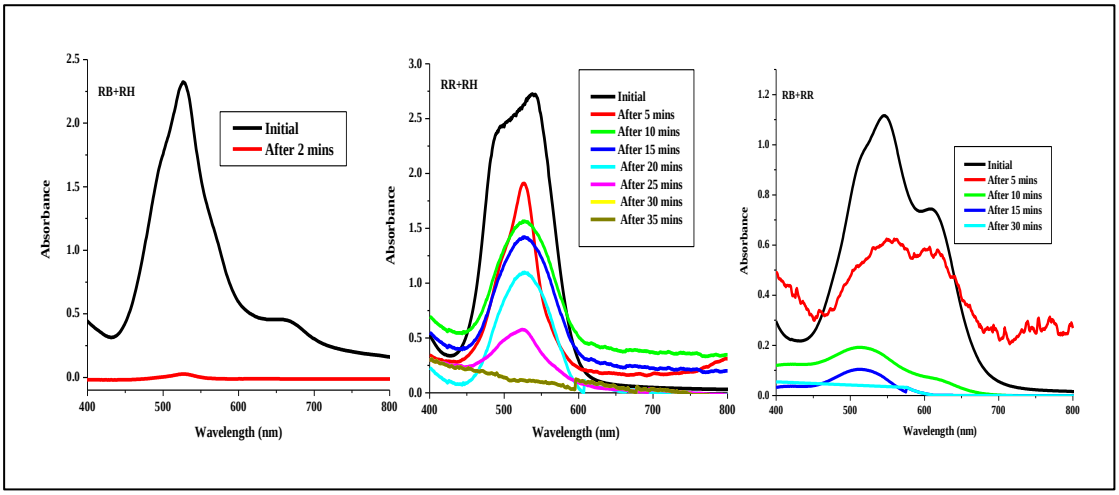

Figure 3.14 UV spectra for degradation of mixture of dyes using CIO as a catalyst

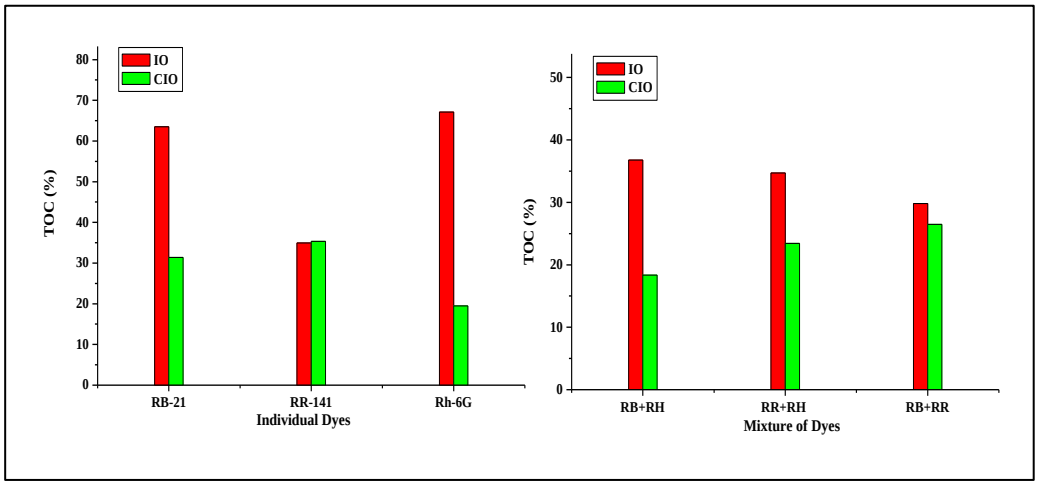

Figure 3.15 TOC for individual and mixture of dyes using IO and CIO as a catalyst

3.4. Mechanism involved in the degradation process

The Fenton's process involves catalytic reaction on the surface of the catalyst producing HO• and HO_2• radicals.The combination of hydrogen peroxide andiron oxide (well-known components of Fenton's reagent) has powerfuloxidizing properties. Hydrogen peroxide reacts with ferrousions to generate active hydroxyl radicals, which mayaccelerate the degradation of dyes. The resulting Fe^{3+} react withhydrogen peroxide to generate a complex ($Fe–O_2H^{2+}$). A simple mechanism for radical formationby Fenton's reagent can be depicted as follows:

$$\mathbf{Fe^{2+} + H_2O_2 \rightarrow Fe^{3+} + HO^{\cdot} + OH^{-}} \quad \text{.....eq. (3)}$$

$$\mathbf{Fe^{3+} + H_2O_2 \rightarrow Fe^{2+} - O_2H^{2+} + H^{+}} \quad \text{.....eq. (4)}$$

$$\mathbf{Fe - O_2H^{2+} \rightarrow Fe^{2+} + HO_2^{\cdot}} \quad \text{.....eq. (5)}$$

$$\mathbf{Fe^{2+} + H_2O_2 \rightarrow Fe^{3+} + HO^{\cdot} + OH^{-}} \quad \text{.....eq. (6)}$$

This hydroxyl radical helps trigger the degradation of dyes.

3.5 Reusability of catalyst

The recovered nanoparticles were recycled three times for degradation offresh individual and mixture of dyes. At the end of each cycle the catalyst was washed with distilled water followed by drying in an oven. For 3 subsequent repetitive cycles, the catalyst showed the same degradation performance as in the case of the initial one.

3.6 Conclusion

Palm shell extract capped iron oxide nanoparticles (IO) and chitosan-ironoxide CIO nanocomposite were synthesised by coprecipitation technique. Characterisation of the synthesised nanomaterials revealed that IO and CIO consisted of mixtures of Fe_3O_4, γ-Fe_2O_3 and α-Fe_2O_3. The nanoparticles were not of uniform size and some of them were small enough to exhibit superparamagnetic properties (SPIONS).The formation of SPIONS was found to be more when embedded in chitosan matrix (CIO). This led to unique mossbauer spectra for CIO which can be attributed to the interaction of chitosan with palm shell extract to form unique encapsulation of the iron oxide particles. CIO showed high catalytic performance towards degradation of individual and mixture of dyes leading to mineralization of the dyes. Furthermore the catalyst could be easily removed and regenerated for the next use.

References

[1] H. Iida, K. Takayanagi, T. Nakanishi, T. Osaka, *J. Colloid Interface Sci*. 314 **(2007)** 274.

[2]] J. Yang, S.B. Park, H.G. Yoon, Y.M. Huh, S. Haam, *Int. J. Pharm*. 324 **(2006)** 185.

[3]] L. Zhou, J. Yuan, W. Yuan, X. Sui, S. Wu, Z. Li, D. Shen, *J. Magn. Magn.Mater*. 321 **(2009)** 2799.

[4] F.X. Hu, K.G. Neoh, E.T. Kang, *Biomaterials* 27 **(2006)** 5725.

[5] M.R. Dhananjeyan, J. Kiwi, K.R. Thampi,*Chem. Commun*. **(2000)** 1443.

[6] J. Fernandez, M.R. Dhananjeyan, J. Kiwi, Y. Senuma, J. Hilborn, *J. Phys. Chem. B* 104 **(2000)** 5298.

[7] M.R. Dhananjeyan, J. Kiwi, P. Albers O. Enea, *Helv. Chim. Acta* 84**(2001)** 3433.

[8] T. Yuranova, L. Garamszegi, J-A. Manson, M. Bensimon, J. Kiwi, *J. Photochem. Photobiol. A.* 150 **(2002)** 195.

[9] J. Feng, X. Hu, P. L. Yue, *Environ. Sci. Technol.* 38**(2004)** 269.

[10] J. Feng, X. Hu, P. L. Yue, *Environ. Sci. Technol.*38 **(2004)** 5773.

[11] B. Sahoo, S. K.Sahu, S. Nayak, D. Dhara, P. Pramanik, *Catal. Sci. Technol.* 2**(2012)**1367.

[12] L. Kao, T. Hsu, K. Cheng, *J. Colloid Interface Sci.* 341 **(2010)**359.

[13] Y. Noda, B. Lee, K. Domen, J. N. Kondo, Chem. Mater. 20 **(2008)** 5361

[14] J. C. Yu, L. Zhang, Z. Zheng, J. Zhao, *Chem. Mater.* 15 **(2003)**

[15] K. Hamada, T. Kaneko, M. Q. Chen, M. Akashi, *Chem. Mater.* 19**(2007)** 1044.

[16] .J. A. Costanzo, C. A. Ober, R. Black, G. Carta, E. J. Fernandez, *Biomaterials*, 2010, 31, 2857

[17] N.J. Tanga, W. Zhonga, H.Y. Jianga, X.L. Wua, W. Liua, Y.W. Du, *J. Magn. Magn.Mater.* 282 **(2009)** 492.

[18] B.J. Palla, D.O. Shah, P. Garcia Casillas, J. Matutes-Aquino, *J. Nanoparticle Res.* 2 **(1999)** 215.

[19] S. Ohta, A. Terada, *Thin Solid Films* 73 **(1986)** 143.

[20] A. Lijuan, L. Zhaoqiang, L. Wei, N. Yaru, C. Zhimin, W. Yanping, Y. Bai, *J. Magn. Magn. Mater*. 303 **(2006)** 127.

[21] J. P. Jolivet,C.Chaneac, E. Tronc, *Chem. Commun.*, 5**(2004)** 481

[22] R. M.Cornell, U.Schwertmann, *The Iron Oxides*; VCH Publishers: Weinheim **(1996)** Germany.

[23] R.Boistelle, J. P. Astier, *J. Cryst. Growth*90**(1988)** 14.

[24] T. Sugimoto, *Chem. Eng. Technol.26***(2003)** 3.

[25] H.-C.Schwarzer, W. Peukert, *Chem. Eng. Commun.* 191**(2004**) 580.

[26] R. M.Cornell, U. Schertmann, *Iron Oxides in the Laboratory:Preparation and Characterization*; VCH Publishers: Weinheim,Germany, 1991.

[27] N. M.Gribanow, E. E. Bibik,O. V. Buzunov, V. N. Naumov, *J.Magn. Magn. Mater*.85 **(1990)** 7.

[28] M. Tominaga, M. Matsumoto,K.Soejima, I. Taniguchi, *J. Colloid Interface Sci.*299**(2006)** 761.

[29] S. E. Khalafalla, G. W. Reimers, *IEEE Trans. Magn.16***(1980)** 178

[30] L.Babes,B. Denizot,G. Tanguy,J. J. L. Jeune, P. Jallet, *J. ColloidInterface Sci.* 212 **(1999)** 474

[31] R. Massart, *IEEE Trans. Magn.*17 **(1981)** 1247.

[32] R. Massart, V. Cabuil, *J. Chim. Phys.84* **(1987)** 7.

[33] J. C. Bacri,R. Perzynski, D. Salin,V. Cabuil, R. Massart, *J. Magn.Magn. Mater.* 85**(1990)**27.

[34] R. Massart, J. Roger, V. Cabuil, *Braz. J. Phys.2* **(1995)** 135.

[35] S.N. Prin,V. Cabuil, R. Massart, P. Escaffre, J. Dussaud, *J. Magn. Magn. Mater.* 122**(1993)** 42.

[36] N. Fauconnier, A. Bee,J. Roger, J. N. Pons, *Prog. Colloid Polym. Sci.*100**(1996)** 212.

[37] N. Fauconnier, A. Bee,J. Roger, J. N. Pons, *J. Mol. Liq.* 83**(1999)** 233.

[38] Fauconnier, N.; Pons, J. N.; Roger, J.; Bee, A. *J. Colloid Interface Sci.* 194**(1997)** 427.

[39] J.Roger,J. N. Pons,R. Massart,A. Halbreich, J. C. Bacri, *Eur. Phys. J. Appl. Phys.5* **(1999)** 321.

[40] B. Denizot, G. Tanguy,F. Hindre, E. Rump,J. J. L. Jeune, P. Jallet, *J. Colloid Interface Sci.*209 **(1999)** 66.

[41] D. Portet, B. Denizot, E. Rump, F. Hindre, J. J. L. Jeune, P. Jallet, *Drug De*V. *Res.*54 **(2001)** 173.

[42] P. H. Mutin, G. Guerrero, A. *C. R* .Vioux, *Chim.6* **(2003)** 1153.

[43] D. I. Kreller, G. Gibson,W. Novak,G. W. V. Loon,J. H. Horton, *Colloids Surf., A*212 **(2003)** 249.

[44] C.Yee,G. Kataby, G. Ulman,T. Prozorov, H. White,A. King,M.Rafailovich, J.Sokolov, A. Gedanken, *Langmuir*15**(1999)** 7111.

[45] J. P. Jolivet, P. Belleville, E. Tronc, J. Livage, *Clays Clay Miner.*40**(1992)**531.

[46] E. Tronc, P. Belleville, J.P. Jolivet, J. Livage, *Langmuir* 8**(1992)** 313.

[47] Sun, S.; Zeng, H. J. Am. Chem. Soc. 124 **(2002)** 8204.

[48] R. M.Cornell, U. Schertmann, *The Iron Oxides:* VCH Publishers: Weinheim, **(1996)**Germany.

[49] Y.Sahoo,H. Pizem,T. Fried,D. Golodnitsky,L. Burstein,C. N.Sukenik, G. Markovich, *Langmuir* 17**(2001)** 7907.

[50] D.Rabelo,E. C. D. Lima,A. C. Reis,W. C. Nunes,M. A. Novak,V. K. Garg,A. C. Oliveira, P. C. Morais, *Nano. Lett.*,1**(2001)** 105.

[51] H.Pardoe,W. C. Anusorn,T. G. St. Pierre, J. Dobson, *J. Magn.Magn. Mater.*225**(2001)** 41.

[52] H.Honda,A. Kawaba,M. Shinkai, T. J. Kobayashi, *Ferment.Bioeng.* 86**(1998**) 191.

[53] A. K. Gupta, M. Gupta, *Biomaterials*26 **(2005)** 3995.

[54] D. K.Kim,W. Voit, W. Zapka, B. Bjelke, M. Muhammed, K. V. Rao, *Mat. Res. Soc. Symp. Proc.*676**(2002)** 8321.

[55] A. K.Gupta, M. Gupta, *Biomaterials*26**(2005)** 3995.

[56] A. Ito, M. Shinkai, H.Honda, T.Kobayashi, *J. Biosci. Bioeng.*100**(2005)** 1.

[57] L.LaConte, N. Nitin, G. Bao, *Nanotoday*8**(2005)** 32.

[58] P.Tartaj,M. P. Morales, T.G. Carren˜o,S. V.Verdaguer, C. J. Serna, *J. Magn. Magn. Mater.* 290-291**(2000)** 28.

[59] H.Pardoe,W. C. Anusorn, T. G. St. Pierre, J. Dobson, J. *Magn.Magn. Mater*. 225**(2001)** 41.

[60] L. F. Gamarra, G. E. S. Brito,W. M. Pontuschka, E. Amaro,A. H. C. Parma, G. F. Goya, *J. Magn. Magn. Mater.* 289**(2005)** 439.

[61] Z.Cao,S. Zhou,J. Liu, X. Song, *Chin. Ger. J. Clin. Oncol.* 4**(2005)** 183.

[62] H. L.Duan, Z. Q.Shen, X. W. Wang, F .-H. Chao, J. W. Li, *World J. Gastroenterol.*11**(2005)** 3660.

[63] D. Bonacchi, A. Caneschi, D. Gatteschi, C. Sangregorio, R. Sessoli, A. Falqui, *J. Phys. Chem. Solids 65***(2004)** 719.

[64] H. Honda, A. Kawaba, M. Shinkai, T. J. Kobayashi, *Ferment. Bioeng.* 86 **(1998)** 191.

[65] F. Llanes, C. Diaz, H. Ryan, R. H. Marchessault, *Int. J. Polym.Mater.* 51**(2002)** 537.

[66] F.L lanes,C. Diaz,H. Ryan, R. H. Marchessault, *Int. J. Polym.Mater.* 51**(2002)** 537.

[67] D. K. Kim, W. Voit, W. Zapka, B. Bjelke, M. Muhammed, K. V. Rao, *Mat. Res. Soc. Symp. Proc.* 676**(2002)** 8321.

[68] F.L lanes, C. Diaz,H. Ryan, R. H. Marchessault, *Int. J. Polym.Mater.* 51**(2002)** 537.

[69] F.Jones,H. Colfen, M. Antonietti, *Colloid Polym. Sci.* 278**(2000)**491.

[70] P.Sipos,T. G. St. Pierre,E. Tombacz, J. Webb, *J. Inorg. Biochem.*58 **(1995)** 129.

[71] Z. Yu, X. Zhang, Y. Huang,, *Ind. Eng. Chem. Res.* 52 **(2013)**11956.

[72] F.Jones, H. Colfen, M. Antonietti, *Biomacromolecules*1**(2000)**556.

[73] F.Jones, H. Colfen, M. Antonietti, *Colloid Polym. Sci.*278**(2000)** 491.

[74] S. Zhou, J. Sun, L. Sun, Y. Dai, L. Liu, X. Li, *Journal of Biomedical Materials ResearchPart B: Applied Biomaterials* 87 **(2008)** 189.

[75] H. Zhao, J. Gagnon, U.O. Hafeli, *Biomagnetic Research and Technology* 5 **(2007)** 2.

[76] T.Y. Liu, S.H. Hu, D.M. Liu, S.Y. Chen, I.W. Chen, *Nano Today* 4 **(2009)** 52

[77] M. Lattuada, T.A. Hatton, *Langmuir* 23 **(2007)** 2158.

[78] M. Diwan, T.G. Park, *Journal of Controlled Release* 73 **(2001)** 233.

[79] X.Liu, Z.Ma,J. Xing, H. Liu, *J. Magn. Magn. Mater.270,***(2004)** 1.

[80] X. Liu,J. Xing,Y. Guan, G.Shan, H. Liu, *Colloids Surf., A* 238**(2004)** 127.

[81] P. Mulvaney, L. M. L. Marzan, M. Giersig, T. Ung, *J. Mater.Chem.* 10**(2000)** 1259.

[82] P. Tartaj, T.G. Carreno, C. J. Serna, *Langmuir* 18**(2002)** 4556.

[83] P. Tartaj, T.G. Carreno, C. J. Serna, *Adv. Mater.* 13**(2001)** 1620.

[84] S. Santra, R. Tapec, N. Theodoropoulou, J. Dobson,A. Hebard, W. Tan, *Langmuir* 17**(2001)** 2900.

[85] M.Chen,S. Yamamuro, D. Farrell, S. A. Majetich, *J. Appl. Phys.*93**(2003)** 7551.

[86] J.Lin,W. Zhou,A. Kumbhar,J. Fang, E. E.Carpenter, C. J. O'Connor, *J. Solid State Chem.* 159**(2001)**26.

[87] W. L.Zhou,E. E. Carpenter,J. Lin,A. Kumbhar, J. Sims,C. J. O'Connor, *Eur. Phys. J. D* 16**(2001)** 289.

[88] A. M. Morawski, P. M. Winter,K. C. Crowder,S. D. Caruthers,R. W. Fuhrlop, M. J.Scott,J. D. Robertson, D. R. Abendschein, G. M.Lanza, S. A. Wickline, *Magn. Reson. Med.* 51**(2004)** 480.

[89] P. G.Shepherd,J. Popplewell, S. W. Charles, *J. Phys. D: Appl.Phys.* 3**(1970)**1985.

[90] H. K.Xu,C. M. Sorensen,K. J. Klabunde, G. C. Hadjipanayis, *J.Mater. Res.* 7**(1992)** 712.

[91] M. D.Alcala, C. Real, *Solid State Ionics* 177(**2006**) 955.

[92] Y. Gushikem, S. S. Rosatto, *J. Braz. Chem. Soc.* 12**(2001)** 695.

[93] K. Woo, J.Hong, J.-P. Ahn, *J. Magn. Magn. Mater.*293**(2005)** 177.

[94] G. A. V. Ewijk, G. J. Vroege, A. P. Philipse, *J. Magn. Magn.Mater.*201**(1999)** 31.

[95] I. J.Bruce, J.Taylor, M.Todd,M. J. Davies,E. Borioni,C.Sangregorio, T. Sen, *J. Magn. Magn. Mater.*284**(2004)** 145.

[96] D. Ma,J. Guan,F. Normandin,S. Denommee,G. Enright,T. Veres, B. Simard,*Chem. Mater.* 18**(2006)** 1920.

[97] J. H.Yu,C. W. Lee,S. S. Im, J. S. Lee, *Rev. Adv. Mater. Sci.4***(2003)** 55.

[98] S.Sun,C. B. Murray,D. Weller, L.Folks, A. Moser, *Science*287**(2000)** 1989.

[99] M. M. Miller, G. A. Prinz, S. F. Cheng, S. Bounnak, *Appl. Phys.Lett.*81**(2002)** 2211.

[100] T. K.Jain,M. A. Morales,S. K. Sahoo,D. L. L. Pelecky, V. Labhasetwar, *Mol. Pharm.* 2**(2005)** 194.

[101] I. Chourpa, L. D. Eyrolles, L. N. Okassa, J. F. Fouquenet, S. C. Jonathan,M. Souce, H.Marchais, P. Dubois, *Analyst* 130 **(2005)** 1395.

[102] J. W. Bulte´, *Methods Mol. Med.*124**(2006)** 419.

[103] M. M. J.Modo, J. W. M. Bulte´, *Molecular and Cellular MR Imaging*; CRC Press: Boca Raton, **(2007)**FL.

[104] S. W.Charles, J. Popplewell, *Endeavour* 6**(1982)** 153.

[105] A. K.Gupta, M. Gupta, *Biomaterials*26 **(2005**) 3995.

[106] M.Chastellain, A. Petri,A. Gupta,K. V. Rao, H. Hofmann, *Adv.Eng. Mater.*, A6, **(2004)** 235.

[107] B. V.Derjaguin, L. Landau, *ActaPhysicochim. URSS* 14**(1941)** 633.

[108] E. J. W.Verwey, J. T. G. Overbeek, *Theory of the Stability ofLyophobic Colloids*; Elsevier: The Netherlands, **(1948)**Amsterdam.

[109] B.Vincent, J. Edwards, S.Emment, A. Jones, *Colloids Surf*. 18**(1986)** 261.

[110] D.Hogemann, L. Josephson, R. Weissleder, J. P.Basilion, *Bioconjugate Chem.* 11**(2000)** 941.

[111] P. Wunderbaldinger, L. Josephson, R. Weissleder, *Acad. Radiol*.9**(2002)**304.

[112] E. H. Kim, H. S. Lee, B. K. Kwak, B. K. Kim, *J. Magn. Magn.Mater.*289**(2005)** 328.

[113] H. S.Lee,E. H. Kim,H. Shao, B. K. Kwak, *J. Magn. Magn. Mater.*293**(2005)**102

[114] G. D.Moeser, W. H. Green, P. E.Laibinis, P.Linse, T. A. Hatton, *Langmuir*20**(2004)** 5223.

[115] R. S.Underhill, G. Liu, *Chem. Mater.*12**(2000)** 2082.

[116] A. M. Awwad, N. M. Salem, *Nanoscience and Nanotechnology*, 2 **(2012)** 208.

[117] S.J. Jun, S. Kim, J.H. Han, *J. Kor. Ceram. Soc.* 35**(1998)** 209.

[118] M. Sastry, A. Ahmad, M.I. Khan, R. Kumar, Curr. Sci. 85 **(2003)** 162.

[119] R.Sanghi,P.Verma,*Bioresour.Technol*.100**(2009)**501.

[120] T. Saito, Y. Nishiyama, J.-L. Putaux, M. Vignon, and A. Isogai, *Biomacromolecules*, 7 **(2006)** 1687.

[121] Y. Zihan, X. Zhang, Y. Huang, *Ind. Eng. Chem. Res*. 52**(2013)** 11956.

[122] JSPDS Data Cards; International Center of Diffraction Data: Swarthmore **(1988)**PA.

[123] M.Liu,C. Chen,J. Hu, X.L. Wu, *J. Phys. Chem*. C. 115**(2011)**25234.

[124] A. A. Dameron, D. Seghete, B. B. Burton, S. D. Davidson, A. S. Cavanagh, J. A. Bertrand, S. M. George, *Chem. Mater*. 20**(2008)** 3315.

[125] K. W. Kwon, B. H. Lee, M. Shim, *Chem. Mater*. 18 **(2006)** 6357.

[126] K. V. P. M.Shafi,A. Ulman,A. Dyal,X. Yan,N. L. Yang,C.Estournes,L. Fournes, A.Wattiaux,H. White, M. Rafailovich, *Chem. Mater.* 14**(2002)**1778.

[127] L. Sun et al. *Materials Science and Engineering C* 30 **(2010)** 583.

[128] Y. Wang, B. Li, Y. Zhou, D. Jia, Y. Song, *Polym. Adv. Technol.* 22 **(2011)** 1681.

[129] M. Wun et al. *Synthetic Metals* 78 **(1996)** 27.

[130] M. Aronniemi et al. *Applied Surface Science* 253 **(2007)** 9476.

[131] S.R.Chowdhury, E.K. Yanful, A.R. Pratt,*J. Hazard. Mater.* **(2012)**235.

[132] M.F.Hochella,.*Rev. Mineral. Geo-chem.* 18 **(1988)**573.

[133] I. Nedkov, L. Slavov, B. Blagoev, K. Krezhov, *Bulg. J. Phys.* 40 **(2013)** 348.

[134] S. MORUP, H. TOPSOE and J. LIPKA, *J. Phys. Colloques*37 **(1976)**287.

[135] M. Siddique, E. Ahmed, N.M. Butt, *Physica B: Condensed Matter* 405 **(2010)**3964.

[136] Shenoy, G. K. *In Mossbauer Spectroscopy Applied to Inorganic Chemistry*; Ed.; Plenum Press: 1**(1984)** 57New York.

[137] B. D. Dunlap, G. M. Kalvius, In *Mossbauer Isomer Shifts***(1978)** 15Amsterdam.

[138] D. Guenzburger, D. M. S. Esquivel, Danon, *J. Phys. ReV. B* 18 **(1978)** 4561.

[139] L.J. Gary, H. Dimitri, A. Mohan , T. Hughbanks ,Xiaobing, F. Grandjean, *J. Am. Chem. Soc.* 120 **(1998)**12163.

[140] S.C. Bhatia, N. Ravi, *Biomacromolecules* 1 **(2000)** 413.

[141] S.C. Bhatia, N. Ravi, *Biomacromolecules* 4 **(2003)** 723.

[142] M. T. Klepka, N.Nedelko, J. M.Greneche, K. L. Jablonska, I. N. Demchenko, A. S. Waniewska, C. A. Rodrigues, A. Debrassi, C. Bordini, *Biomacromolecules 9***(2008)** 1586.

[143] Y. Ding, Y. Hu, L. Zhang, Y. Chen,X. Jiang, *Biomacromolecules* 7 **(2006)** 1766.

[144] A. L. D. Silva, T. Trindade, B. J. Goodfellow, B. F. O. Costa, R. N. Correia, A. M. Gil, *Biomacromolecules* 8**(2007)** 2350.